ELSEVIER

Journal of Photochemistry and Photobiology A: Chemistry 119 (1998) 47–52

Journal of Photochemistry and Photobiology A:Chemistry

Photochemical consequences of porphyrin and phthalocyanine aggregation on nucleoprotein histone

K. Lang[a,*], P. Kubát[b], J. Mosinger[a], D.M. Wagnerová[a]

[a]*Institute of Inorganic Chemistry, Academy of Sciences of the Czech Republic, 250 68, Řež, Czech Republic*

[b]*J. Heyrovský Institute of Physical Chemistry, Academy of Sciences of the Czech Republic, Dolejškova 3, 182 23, Praha 8, Czech Republic*

Received 25 June 1998; accepted 25 August 1998

Abstract

Anionic photosensitizers, meso-tetrakis(4-sulfonatophenyl)porphyrin (TPPS) and chloroaluminium phthalocyanine tetrasulfonate (AlPCS), are bound to histone by Coulombic attraction as has been evidenced by absorption and fluorescence spectra. At variance to serum albumins, histone promotes aggregation of the bound monomeric sensitizer, the apparent dimerization constants being $K_D = 4.2 \times 10^5\ M^{-1}$ ($\pm 0.4 \times 10^5$) and $3.3 \times 10^5\ M^{-1}$ ($\pm 0.7 \times 10^5$) for TPPS and AlPCS, respectively. Hydrophobic environment and the shielding effect of positively charged histone act as self-aggregating driving forces for the formation of stacked aggregates. Sensitizer–histone ground state interactions and their influence on photophysical properties have been analyzed. Reduction of the triplet quantum yields Φ_T induced by aggregation on histone considerably decreases the sensitizing ability. The bimolecular rate constant for quenching of histone bound triplet ^{3}TPPS by oxygen is $(3.9 \pm 0.7) \times 10^8\ M^{-1}\ s^{-1}$, which is one order of magnitude lower than that for the free sensitizer.

Keywords: Porphyrin; Phthalocyanine; Histone; Aggregation; Photosensitization; Excited states

1. Introduction

Application of singlet oxygen producing photosensitizers phthalocyanines and porphyrins in photodynamic therapy posed a question: How will proteins and DNA change photochemical and photophysical properties of the sensitizers and subsequent photoinduced reactions. It has been reported that human [1–4] and bovine serum albumins [5] non-covalently bind anionic sensitizers like sulfonated porphyrins and phthalocyanines. The formation of albumin-sensitizer adducts affects natural singlet and triplet lifetimes and rate constants of subsequent processes as quenching of the excited triplet states by oxygen. Ground state interactions between the sensitizer and the protein have been shown to be essential for elucidation of these effects. Therefore, studies focused on molecular interactions between sensitizers and constituents of biological systems are of utmost interest.

Nucleoproteins histones play a key role in the compaction of DNA. DNA is wound around a core of eight histone units forming a DNA–protein complex called chromatin [6,7]. The five types of histones range in mass from 11 to 21 kD. With respect to their basic character, i.e. high content of either lysine or arginine residues with positively charged side chains, strong electrostatic attraction of anionic sensitizers can be expected. Histones are supposed to be more resistant to oxidative attack of singlet oxygen produced in situ [8] than albumins because, of the readily oxidizable amino acid residues, histones contain no Trp and little or no Cys, Met and His [7,9]. In spite of the evident importance of histones in the context of the photodynamic effect, their influence on exogeneous sensitizers has not been reported so far.

In this paper we report behavior of two sensitizers suggested for photodynamic therapy of tumors – tetrakis (4-sulfonatophenyl)porphyrin (TPPS) and chloroaluminium phthalocyanine tetrasulfonate (AlPCS) in the presence of histone. Sensitizer–histone ground state interactions and their influence on photophysical properties have been analyzed.

2. Experimental details

5,10,15,20-Tetrakis(4-sulfonatophenyl)porphyrin tetrasodium salt (Aldrich), 5,10,15,20-tetrakis(4-carboxyphenyl)-

*Corresponding author.

1010-6030/98/$ – see front matter
PII: S1010-6030(98)00380-3

porphyrin, TPPC, (Porphyrin Products), 5,10,15,20-tetrakis(4-*N*-methylpyridyl)porphyrin tetraiodide, TMPyP, (Strem Chemicals), chloroaluminium phthalocyanine tetrasulfonate (Porphyrin Products), bovine serum albumin, BSA, (fraction V, Merck), and arginine-rich histone H3 from calf thymus (Johns fraction III, Fluka) were used as received.

The experiments were performed either in a phosphate buffer of pH 7.20 and 5.70 or in an acetate buffer ($I = 0.015$) of pH 3.48. In some experiments the ionic strength was regulated by NaCl (up to 1 M). If necessary, especially at pH 7.20, small amounts of undissolved histone from freshly prepared solutions were removed on a Millipore filter (0.45 μm). UV/Vis spectra were recorded on a Perkin Elmer Lambda 10 or a Philips PU 8720 spectrophotometers. Difference absorption spectra were measured for sensitizer/histone (ca. 3 μM) solutions vs. equal concentration of the sensitizer in excess of BSA. In BSA solutions sensitizer–BSA ratio R was kept under 0.2 to ensure BSA bound monomer to dominate.

Fluorescence experiments were carried out on a Perkin Elmer LS 50B luminescence spectrometer. The samples had equal absorbance ($A < 0.05$, 1 cm cell) at the excitation wavelengths of 519 nm (TPPS) or 630 nm (AlPCS). Fluorescence quantum yields Φ_f were estimated by comparison of fluorescence intensities in the presence and absence of histone. Light-scattering experiments were conducted using simultaneous scans of the excitation and emission monochromators through the range of 300–600 nm.

Laser flash photolysis experiments were performed with a Lambda Physik FL 3002 dye laser (excitation wavelengths: 413 nm for porphyrins, 658 nm for AlPCS) pumped by a Lambda Physik LPX 200 excimer laser (308 nm, output 2 mJ/pulse, pulse width ~28 ns). The triplet states were probed at absorption maxima of ^{3}TPPS (450 nm) and ^{3}AlPCS (490 nm) using a 250 W Xe lamp equipped with a pulse unit and a R928 photomultiplier. Oxygen was removed by purging the solution with argon. BSA and histone cause foaming that increases the error of the triplet lifetimes up to 20%.

A piezoelectric transducer, connected with a home-made preamplifier and a LeCroy 9621 oscilloscope, served as a detector for laser-induced optoacoustic spectroscopy (LIOAS). We used buffered solutions of pH 7.20 with TPPS–histone ratio R ranging from 0 to ~0.2. The samples were air-saturated because purging the solution with argon in order to remove oxygen is accompanied by extensive foaming. An excitation wavelength of 420 nm was chosen because at this wavelength the absorbance is identical for all samples and amounts to $A_{420} = 0.350 \pm 0.010$. The fraction of absorbed energy released as prompt heat α for TPPS solutions was obtained from linear optoacoustic amplitude vs. incident energy plots and by comparison with a calorimetric reference $(NH_4)_2CrO_4$ with $\alpha = 1.0$ [10]. The effective acoustic transit time τ_a' was set at 0.7 μs (pinhole of 1 mm diameter). Singlet oxygen was determined using time-resolved near infrared emission at 1270 nm. Optically-matched air saturated TPPS (5 μM) – a reference sensitizer – and TPPS/histone solutions in D_2O were excited by the Lambda Physik FL 3002 dye laser (varying between 402 and 420 nm for TPPS, 658 nm for AlPCS) as described elsewhere [11]. Emission was monitored at right angle to the excitation beam with a Ge diode (Judson J16-8SP-R05M-HS,USA). The quantum yields of singlet oxygen formation Φ_Δ were estimated by comparing the slopes of emission amplitude vs. the laser fluence.

3. Results

3.1. Association of sensitizers with histone

Spectral properties of TPPS and AlPCS were investigated in the range 250–700 nm as a function of concentration. The low tendency of TPPS and AlPCS to aggregate [12–14] is evidenced by absorption and fluorescence spectra collected for micromolar concentrations.

Addition of histone to TPPS evokes marked spectral changes that reveal binding of porphyrin and binding-induced alteration of sensitizer physico-chemical properties. The Soret band at 414 nm (Fig. 1(g)) is broadened and split into two maxima 405 and 420 nm (Fig. 1(a)–(f)), accompanied by considerable hypochromicity and deviations from the Beer's law. The molar absorption coefficient at 420 nm decreases with increasing porphyrin–histone ratio R (Fig. 1, inset). The Q bands in the visible region are red shifted (Table 1). A red shift is observed also for fluorescence emission peaks (Table 1, Fig. 2(a) and (c)). In addition, interaction of TPPS with histone causes a decrease of intensity of both excitation and emission spectra characterized by low Φ_f of 0.035. That is almost one half of Φ_f measured for free TPPS [13] (Table 2). However, similar to free TPPS at neutral pH, the Q(0,0) and Q(0,1) peaks are independent of excitation wavelength.

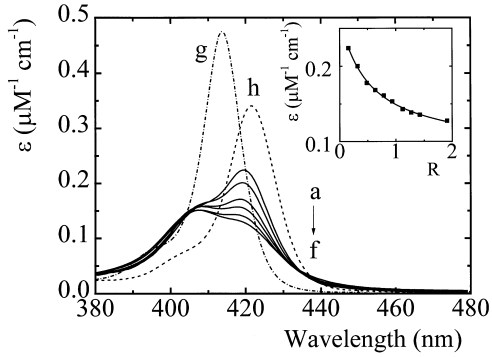

Fig. 1. Absorption spectra of TPPS in the Soret region; (a)–(f): R (porphyrin/histone) = 0.16, 0.32, 0.64, 0.78, 1.27 and 1.90. With increasing R the observed ϵ at 420 nm decreases (see inset). Phosphate buffer pH 5.70 (7 mM), 3.3 μM histone. Absorption spectra of 1.8 μM TPPS (g) and of the TPPS–BSA adduct, $R = 0.16$ (h). Phosphate buffer pH 7.20 (7 mM).

Table 1
Spectroscopic data of TPPS and AlPCS. The formulas used for the attached sensitizers do not characterize the stoichiometry of the adducts but denote the form of the sensitizer on the protein(log ϵ/M^{-1} cm^{-1})

Compound	Absorption spectrum λ_{max}/nm					Fluorescence spectrum λ_{max} /nm	
TPPS	414 (5.65)	516 (4.20)	553 (3.83)	580 (3.81)	633 (3.57)	646	704
TPPS–histone		519 (4.08)	555 (3.63)	593 (3.66)	650 (3.52)	656	722
$TPPS_{agg}$–histone	405[a]					not resolved[b]	
TPPS–BSA	422 (5.53)	519 (4.20)	553 (3.91)	592 (3.78)	646 (3.59)	653	718
AlPCS	351 (4.78)	607 (4.47)	674 (5.25)			686	718
AlPCS–histone	350		673			688	755
$AlPCS_{agg}$–histone		627[a]	656[a]			not resolved	
AlPCS–BSA	351 (4.72)	609 (4.46)	676 (5.26)			689	752

[a]From difference absorption spectra.
[b]TPPS–histone has much higher Φ_f than $TPPS_{agg}$–histone. Very low fluorescence emission of $TPPS_{agg}$–histone is probably at 680 and 750 nm as follows from excitation fluorescence spectra.

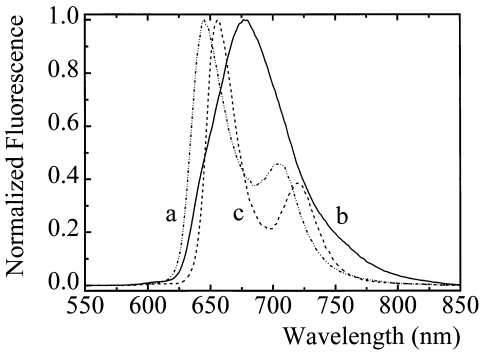

Fig. 2. Normalized fluorescence spectra of TPPS using $\lambda_{exc} = 519$ nm (a) and of protonated H_2TPPS using $\lambda_{exc} = 430$ nm (b) of the same sample. Fluorescence spectra in the presence of 3.3 μM histone using $\lambda_{exc} = 510$ nm (c) independent of excitation wavelength. Phosphate buffer pH 5.70 (7 mM), 1.8 μM TPPS.

Spectral features of the TPPS/histone system confirm the presence of several spectroscopically distinguishable porphyrin forms. It can be excluded that the porphyrin located in different regions of histone has different absorption spectra. In such a case the absorption maxima in the visible region (500–680 nm) would depend on R, which was not observed. Excitation fluorescence spectra exhibit wavelength dependency: two distinct peaks at 408 and 419 nm arise when emission wavelengths of 679 (also 750) and of 646 nm (also 722 nm) have been used. The latter peak at 419 nm is typical for monomeric porphyrin bound on a protein like BSA (Table 1). The statement that TPPS is monomeric and forms an adduct TPPS–BSA is based on our spectroscopic analysis up to $R = 1.19$ and on studies of porphyrin and phthalocyanine affinity to serum albumins [1,5,15,16]. A parallel between the position and relative heights of absorption bands and fluorescence emission peaks of monomer bound to histone and to BSA shows that the hydrophobic microenvironment of both proteins has the same effect on spectral properties (Table 1, Fig. 1(a) and (h)). Since the binding-induced spectral changes are better visualized by difference absorption spectra (Fig. 3), histone solutions of $R < 2$ were recorded against BSA solutions with equal concentration of TPPS in the form of the TPPS–BSA adduct. The isosbestic point at 413 nm indicates an equili-

Table 2
Excited state properties of TPPS in the absence and presence of histone and BSA

	Histone	BSA	Solution
Emission maximum $Q(0,0)$	656 nm	653 nm	646 nm, 675 nm[a]
Fluorescence quantum yield	0.035[b]	–	0.060±0.005[c]
Triplet absorption maximum	450 nm	450 nm	450 nm
Triplet quantum yields	≤0.2[d]	–	0.76±0.08[e]
Triplet lifetime	1000 μs[f]	2400 μs[f]	510 μs[g]
Quantum yields of $^1O_2$	<0.1[h]		0.57±0.14[i]
k_q ($M^{-1}s^{-1}$)	$(3.9\pm0.7) \times 10^8$	$(4.7\pm0.5) \times 10^8$	$(1.8\pm0.1) \times 10^9$

[a]Protonated H_2TPPS.
[b]±10%, $R = 0.55$.
[c]Reference [13].
[d]$R \sim 0.2$.
[e]Reference [28].
[f]Error 20%.
[g]Reference [8], error 6%.
[h]$R \sim 1$.
[i]Average literature value [29].

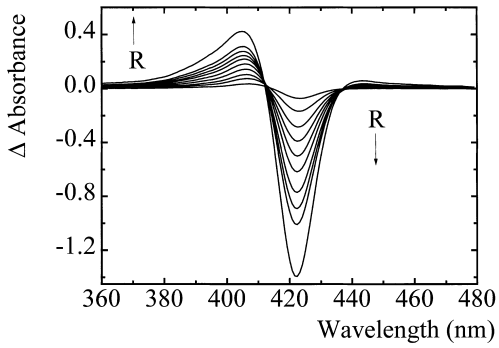

Fig. 3. Difference absorption spectra of TPPS in the presence of histone measured vs. monomer of TPPS bound to BSA (TPPS–BSA). Increasing R from 0.16 to 1.91 is indicated by the arrow. The isosbestic point is at 413 nm. Phosphate buffer pH 5.70 (7 mM), ca. 3.3 μM histone.

brium between two species. The subtraction of the monomer peak from the total envelope of absorption spectra enables spectral characterization of a second form which differs from bound monomer. Within the studied range of R, we have evidence that the total amount of TPPS is accommodated on histone and the equilibrium demonstrated by Fig. 3 is not established between free (uncomplexed) and bound sensitizer, as has been generally found for albumins [1,5,15,16]. The concentration of bound TPPS monomer (TPPS–histone) that has typical absorption peak about 420 nm decreases with higher R (Fig. 1, inset), concomitant with increasing contribution of a second form. The second form has a differential peak at 405 nm that is characteristic for porphyrin aggregates. Hence, we infer that the equilibrium is established between TPPS–histone and a porphyrin aggregate buried in histone. We denote this aggregate as $TPPS_{agg}$–histone. Having employed the resonance light scattering method [17], we did not find any enhancement of scattered light intensity that is indicative of very large aggregates.

The complete depletion of free TPPS in the presence of histone has interesting implications. At pH 3.48 and pH 5.70, two porphyrin nitrogens are protonated to form the dianion H_2TPPS ($pK_a = 4.8$). When histone is added (examined up to $R = 0.6$), the absorption peaks at 435, 647, and the emission peak at 680 nm (Fig. 2(b)), belonging to protonated H_2TPPS, are fully substituted by above described porphyrin–histone spectra (Fig. 2(c)). It means that H_2TPPS disappears from solution and only unprotonated TPPS is accommodated on the protein.

Increasing ionic strength leads to liberation of TPPS from histone adducts. This is indicative of electrostatic attraction between negatively charged peripheral substituents of TPPS and positively charged binding sites of histone. At pH 3.48 and [NaCl] > 0.60 M, liberation ends by formation of J-aggregates of TPPS regardless of the presence of histone.

On addition of histone or BSA, AlPCS behaves similarly to TPPS (Table 1). BSA accommodates two molecules of monomeric AlPCS [5]. Differential absorption spectra of AlPCS and histone measured against the AlPCS–BSA adduct have four isosbestic points in the visible region at 599, 614, 662, and 697 nm. Two differential bands that appear at 607 and 679 nm are characteristic of phthalocyanine monomers [5,18–20] and are attributed to a monomer–histone adduct (AlPCS–histone). On the other side, two peaks at 627 and 656 nm are similar to those of phthalocyanine aggregates in solution [18–20]; their intensities grow with increasing R. We attribute them to phthalocyanine aggregated on histone denoted as $AlPCS_{agg}$–histone. Thus, on the bases of absorption and fluorescence spectra, we conclude that monomeric AlPCS (AlPCS–histone) and aggregated AlPCS ($AlPCS_{agg}$–histone) are non-covalently attached to histone; free AlPCS has not been detected. Aggregation is accompanied by 70% quenching of AlPCS fluorescence when compared to fluorescence of AlPCS monomer on BSA (AlPCS–BSA).

Interaction with histone is governed by the sensitizer's negative charge. Both TPPS and AlPCS have peripheral sulfo groups and therefore the molecules are in fact tetravalent anions. The concentration range for investigation of sensitizer–histone interactions is limited by precipitation of histone occurring for $R > 2$. This can be explained by protein compaction caused by the excess of the multifunctional sensitizers. Substitution of TPPS by TPPC bearing four carboxy groups does not affect the above described behavior. In contrast, positively charged porphyrin TMPyP does not show any sign of interaction with histone and of precipitation (examined up to $R = 4.0$).

3.2. Laser flash photolysis

The properties of the excited singlet and triplet states of TPPS as well as the effects of histone and BSA are summarized in Table 2. The kinetics of ^{3}TPPS decay and of ^{3}TPPS quenching by oxygen slows down after addition of histone. Even though the shape of triplet–triplet absorption spectrum is not changed, its intensity is considerably reduced with increasing R (Fig. 4). It implies that the quantum yields of triplet formation Φ_T decrease as a result

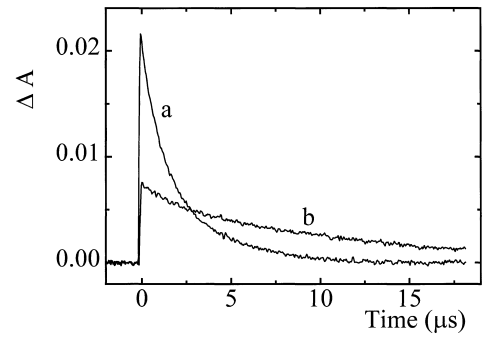

Fig. 4. Transient kinetic traces following 413 nm laser pulse excitation of 1.8 μM TPPS in the absence (a) and in the presence of ca. 3.4 μM histone (b). Phosphate buffer pH 5.70 (7 mM), absorbance measured at 450 nm. Air saturated.

of TPPS aggregation (vide supra). The lifetime of ^{3}TPPS doubles from 510 μs to 1000 μs. Quenching of histone bound monomer ^{3}TPPS by oxygen is characterized by a single bimolecular rate constant k_q of $(3.9 \pm 0.7) \times 10^8\ M^{-1}\ s^{-1}$ that is about one order of magnitude lower than that of free ^{3}TPPS (Table 2, Fig. 4). The decrease results from less effective collisional quenching. For comparison, oxygen quenching of ^{3}TPPS in the presence of BSA cannot be represented by a single exponential process as in the case of histone, but is well described by a two-exponential model involving free and complexed sensitizer in equilibrium [5].

Protonation of free ^{3}TPPS occurs at pH $\leq$ 5.70 and is manifested by biexponential course of oxygen quenching because both unprotonated and protonated triplet states have different rate constants. In the presence of histone (or BSA) only unprotonated triplets of bound monomer, i.e. ^{3}TPPS-histone were detected. At medium pH, the growth of the monoacid ^{3}HTPPS concentration generated from ^{3}TPPS can be monitored at 500 nm [8]. Histone (or BSA) hinders protonation. The described behavior shows that the porphyrin is located in the area of reduced accessibility to water molecules. It is in line with our finding deduced from absorption and fluorescence spectra (vide supra).

The quantum yields Φ_T were measured using LIOAS. With respect to time-limited stability of histone solutions and to contributions of TPPS monomer and aggregate varying with changing R, we estimated the upper limit of Φ_T. The quantum yields of singlet oxygen formation Φ_Δ were found to be under detection limit, $\Phi_\Delta < 0.1$, as no phosphorescence of $^1O_2$ was observed at $R \sim 1$. Entering the values from Table 2, the molar energy of the excitation light $E_{exc} = 285\ kJ\ mol^{-1}$, the molar energy of the fluorescing state $E_{fl} = 174\ kJ\ mol^{-1}$, the molar energy of $^1O_2$ $E_\Delta = 94\ kJ\ mol^{-1}$, the molar energy of the triplet states $E_T = 139\ kJ\ mol^{-1}$, the lifetime of $^1O_2$ $\tau_\Delta = 3.2$ μs, and the triplet lifetime $\tau_T = 9.5$ μs into the energy balance equation [10] yields for TPPS/histone of $R \sim 0.2$ the fraction $\alpha = 0.66 \pm 0.06$. It means that a higher amount of prompt heat is released within τ_a' compared to monomer in solution where $\alpha = 0.44 \pm 0.05$. From the values of α follow $\Phi_T \leq 0.2$ corroborating the measured decrease of triplet state concentrations (Fig. 4). This is in agreement with our aggregation concept because aggregated compounds exhibit little or no sensitizing ability as a result of efficient radiationless dissipation of absorbed energy. This is generally connected with reduction of Φ_f, Φ_T and Φ_Δ [21,22]. On the contrary, binding of zinc meso-tetrakis(2,6-dichloro-3-sulfonatophenyl)porphyrin to albumin affects neither triplet state formation nor Φ_Δ [1]. We did not determine Φ_Δ for the adduct TPPS–BSA precisely, however, its behavior appears to be identical.

In the presence of histone, AlPCS behaves in the same way as TPPS: k_q is one order of magnitude lower than in the absence of histone, Φ_T is reduced and Φ_Δ is under detection limit (≤ 0.1). No influence of histone on singlet and triplet state properties of TMPyP was observed since TMPyP does not interact with histone.

4. Discussion

Binding of the sensitizer by histone or BSA induces electronic perturbations that are manifested by a red shift of absorption bands of the monomeric complexed sensitizer, when compared to monomer in aqueous solution. The perturbation arises from the changes in the solvent–solute interactions after placing the molecule into hydrophobic environment. Porphyrin monomers and oligomers are accommodated by proteins differing in the number and affinity of binding sites [1,23–25]. Since both sensitizers TPPS and AlPCS are predominantly monomeric in solution, we can exclude direct binding of dimers or higher aggregates by histone. Low extent of porphyrin aggregation on albumins has been reported at ratios R higher than 1 [15,16]. At variance, we report the existence of two sensitizer–histone forms in equilibrium at low $R \sim 0.1$ i.e. under conditions where no aggregation on albumins has been observed. The monomer–histone adduct is expected to have spectral and photochemical properties similar to monomer attached to albumins. The second species behaves spectrally as aggregated TPPS or AlPCS. Apparently, monomer and aggregate are relatively freely attached to histone binding sites so that the equilibrium between them can be established.

Histone possesses high content of positively charged side-chains on the abundant Lys and Arg residues and is prone to aggregation in the presence of multifunctional molecules [26]. It appears that the sensitizers induce such a process. The sensitizer is electrostatically attached on the solvent exposed surface of histone. The four negative charges are not compensated and induce gradual histone compacting leading to high local concentration of the sensitizer in the inner histone volume. Shielding of the negative sulfo groups by positive charges of histone promotes aggregation through π–π interaction of macrocycle units. The result is that the entire amount of the sensitizer is in contact with hydrophobic histone environment and the buried aggregated sensitizer is not attached to specific binding sites. Inhibition of TPPS protonation in the ground and triplet states by histone confirms that the sensitizers are placed in an environment with low activity of water molecules.

The formation of extended sensitizer aggregates has been excluded by light scattering measurement. It implies the limited space in the inner volume of histone. It is likely that at low R dimers are the predominant aggregated form, similarly to dimerized charged porphyrin in bilayers [27]. Presuming a dimerization model [21], simultaneous fitting of the observed molar absorption coefficients in the range 413–425 nm (TPPS) and 630–682 nm (AlPCS) vs. total concentration of the sensitizer, yields the apparent dimerization constants $K_D = 4.2 \times 10^5\ M^{-1}$ ($\pm 0.4 \times 10^5$) and $3.3 \times 10^5\ M^{-1}$ ($\pm 0.7 \times 10^5$), respectively. For comparison,

TPPS in solution has K_D of 4×10^3 M^{-1} [13], i.e. two orders of magnitude smaller. AlPCS in aqueous solutions is believed to be monomeric. Though the model well describes the datasets, it is necessary to introduce corrections for local concentrations in the inner histone volume. The local concentration is much higher than in solution and difficult to estimate. Taking into account that the aggregation number can depend on R one can see that the dimerization model simplifies the real behavior.

Observed quenching of fluorescence is not attributed to an enhancement of efficiency of intersystem crossing since in fact Φ_T decreases. Instead, efficiency increase of internal conversion is suggested due to aggregation of the sensitizers within histone. The Φ_T decrease implies considerable reduction of Φ_Δ since $^1O_2$ production for TPPS and AlPCS occurs only by oxygen quenching of the triplet state sensitizer [29]. In this context we can exclude charge separation processes reported for some porphyrin containing systems because there is neither spectroscopic nor kinetic evidence that the sensitizer excited states donate or abstract an electron from amino acids on the adjacent protein.

We conclude that the organization and distribution of sensitizer molecules non-covalently bound to histone considerably affect sensitizing ability via induced aggregation, quenching of Φ_T and, consequently, Φ_Δ.

Acknowledgements

We wish to acknowledge the support from the Grant Agency of the Czech Republic (grant No. 203/96/1322).

References

[1] J. Davila, A. Harriman, J. Am. Chem. Soc. 112 (1990) 2686.
[2] J. Davila, A. Harriman, Photochem. Photobiol. 51 (1990) 9.
[3] M.S.C. Simpson, A. Beeby, S.M. Bishop, A.J. MacRobert, A.W. Parker, D. Phillips, Time-Resolved Laser Spectroscopy in Biochemistry III, SPIE Proceedings, Vol. 1640, 1992.
[4] D. Phillips, Pure Appl. Chem. 67 (1995) 117.
[5] K. Lang, D.M. Wagnerová, P. Engst, P. Kubát, Z. Phys. Chem. 187 (1994) 213.
[6] V. Karantza, E. Freire, E.N. Moudrianakis, Biochemistry 35 (1996) 2037.
[7] R. DeLange, E.L. Smith, J. Biological. Chem. 248 (1973) 3248.
[8] P. Kubát, K. Lang, J. Mosinger, D.M. Wagnerová, Z. Phys. Chem., in print.
[9] G.R. Tristram, R.H. Smith, in: Neurath (Ed.), The Proteins, Vol. 1, II edition, Academic Press, London, 1963.
[10] S.E. Braslavsky, G.E. Heibel, Chem. Rev. 92 (1992) 1381.
[11] P. Kubát, Z. Zelinger, M. Jirsa, Radiat. Res. 148 (1997) 382.
[12] R.F. Pasternack, P.R. Huber, P. Boynd, G. Engasser, L. Francesconi, E. Gibbs, P. Fasella, G.C. Venturo, L deC. Hinds, J. Am. Chem. Soc. 94 (1972) 4511.
[13] T. Gensch, S.E. Braslavsky, J. Phys. Chem. B 101 (1997) 101.
[14] P.C. Martin, M. Gouterman, B.V. Pepich, G.E. Renzoni, D.C. Schindele, Inorg. Chem. 30 (1991) 3305.
[15] E. Reddi, F. Ricchelli, G. Jori, Int. J. Peptide Protein Res. 18 (1981) 402.
[16] I.E. Borissevitch, T.T. Tominaga, H. Imasato, M. Tabak, J. Lumines. 69 (1996) 65.
[17] R.F. Pasternack, P.J. Collins, Science 269 (1995) 935.
[18] X.-F. Zhang, H.-J. Xu, J. Chem. Soc. Faraday Trans. 89 (1993) 3347.
[19] M.G. Lagorio, L.E. Dicelio, E.S. Román, J. Photochem. Photobiol. A: Chem. 72 (1993) 153.
[20] D.A. Fernández, J. Awruch, L.E. Dicelio, J. Photochem. Photobiol. B: Biol. 41 (1997) 227.
[21] P. Abós, C. Artigas, S. Bertolotti, S.E. Braslavsky, P. Fors, K. Lang, S. Nonell, F.J. Rodríguez, M.L. Sesé, F.R. Trull, J. Photochem. Photobiol. B: Biol. 41 (1997) 53.
[22] C. Tanielian, C. Wolff, M. Esch, J. Phys. Chem. 100 (1996) 6555.
[23] M. Rotenberg, R. Margalit, Biochem. J. 229 (1985) 197.
[24] V. Rosenberger, R. Margalit, Photochem. Photobiol. 58 (1993) 627.
[25] W.T. Morgan, A. Smith, P. Koskelo, Biochim. Biophys. Acta 624 (1980) 271.
[26] C. von Holt, W.F. Brandt, H.J. Greyling, G.G. Lindsey, J.D. Retief, J. de A. Rodrigues, S. Schwager, B.T. Sewell, in: P.M. Wassarman, R.D. Kornberg (Eds.), Methods of Enzymology, Vol. 170, p. 431, Academic Press, 1989.
[27] J.H. van Esch, M.C. Feiters, A.M. Peters, R.J.M. Nolte, J. Phys. Chem. 98 (1994) 5541.
[28] R. Bonnet, R.J. Ridge, E.J. Land, R.S. Sinclair, D. Tait, T.G. Truscott, J. Chem. Soc., Faraday Trans. I 78 (1982) 127.
[29] F. Wilkinson, W.P. Helman, A.B. Ross, J. Phys. Chem. Ref. Data 22 (1993) 113.